

UDC 544.723.21

ON THE CORRELATION BETWEEN CHARACTERISTICS OF CATALYST PARTICLES AND CHANGES IN POROUS STRUCTURE OF ACTIVATED CARBON IN IRON-CATALYZED CARBON HYDROGENATION REACTION

O.N. Stavinskaya

*Chuiko Institute of Surface Chemistry of National Academy of Sciences of Ukraine
17 General Naumov Str., Kyiv, 03164, Ukraine*

The sizes and composition of iron-containing particles formed in pores of activated carbon during heat treatment in flowing hydrogen have been studied by Mossbauer spectroscopy. The changes in porous structure of activated carbon due to iron-catalyzed carbon hydrogenation were investigated by means of adsorption method. With the same percentages of burn-off, the sizes of pores formed in the adsorbent during activation have been found to increase for the sample with higher iron loading and larger catalyst particles.

INTRODUCTION

Presence of well-developed mesopores in porous texture of carbon adsorbents may be desirable in various fields of carbon applications and activation of carbon materials in catalytic processes appears to be a simple way to develop carbons mesoporosity [1]. Gasification of carbon by using a catalyst also seems to give an opportunity to effect the changes in porous texture of carbon adsorbents during activation. In our previous studies [2, 3] on activated carbons containing 10–20 wt.% of iron and hydrogenated at temperature in excess of 500 °C we have found that, under the same treatment conditions, sizes of mesopores generated depended on iron loading and could be affected by low temperature samples pretreatment leading to changes in particles size prior to carbon gasification initiation. The present communication contains some additional data supporting the idea of the correlation between characteristics of catalyst particles and changes in porous structure of activated carbons in the course of iron-catalyzed carbon hydrogenation.

EXPERIMENTAL

Spherically granulated synthetic activated carbon (AC) from a copolymer of styrene and divinylbenzene [4], with a particle size of 0.4–0.6 mm, was used as a starting material for investigation. S1 and S2 samples with iron loading of $C_{Fe} = 5$ and 2 wt. % were prepared by

impregnation of starting carbon with aqueous solutions of iron(III) nitrate of different concentration. After drying in air at room temperature both the samples were heated for 90 min in flowing hydrogen at the pressure of 1 atm and at the temperature of 350 °C, which is less than carbon ignition temperature, and then hydrogenated at 550 and 700 °C.

The study of iron-containing particles was carried out by means of Mossbauer spectroscopy. The Mossbauer spectra were obtained at 80 K with a conventional constant-acceleration spectrometer and ^{57}Co in chromium matrix used as a source. Isomer shifts are presented relative to a metallic iron. The spectra were fitted using the approximation of Lorentzian line shape.

The parameters of porous structure for starting and iron-containing carbons were found from the benzene adsorption isotherms, the total pore volume V_{Σ} of the samples was determined by means of their impregnation with acetone. Volume of micropores V_{mi} and mesopores V_{me} and surface area of mesopores S_{me} were calculated according to the theory of volume filling of micropores for the case of micromesoporous adsorbents [5]; the Broekhoff–de Boer–Dubinin method [6] was used to determine the pore size distribution over radius. Referring the pores to micro- and mesopores was made in accordance with Dubinin's classification of micro- and mesopores (pores with radii $r < 1.5$ – 1.6 nm and 1.5 – $1.6 < r < 100$ – 200 nm,

* corresponding author okstavinskaya@yahoo.com

respectively) [5]. The parameters of porous structure for starting and iron-containing carbons are given per 1 cm³ of the samples.

RESULTS AND DISCUSSION

Figure 1 shows the Mossbauer spectra of S1 sample treated in hydrogen at 350–700 °C; spectra of S2 samples were similar to those of S1 ones and differed from them only by contribution of various signals to the overall spectra. Time of heat treatment at each temperature is 90 min. The following components can be distinguished in the spectra: a doublet with an isomer shift of $\delta = 0.36 \pm 0.05$ mm/s and quadrupole splitting of $\Delta E_Q = 0.83$ – 0.93 mm/s (spectra 1–3); an intensive singlet with isomer shift of $\delta = -0.1 \pm 0.05$ mm/s and linewidth of $\Gamma = 0.29 \pm 0.05$ mm/s (spectrum 3 of the sample treated at 700 °C); a sharp sextet I with hyperfine parameter $H_{\text{eff}} = 340$ kOe (spectra 2, 3) and a broad sextet II with H_{eff} up to 490 kOe (spectra 1–3). In accordance to numerous Mossbauer studies on iron-containing particles of various sizes and structure, the subspectra mentioned above can be assigned, respectively, to small iron oxide particles with diameter $d < 3$ – 5 nm [7–9], to non-magnetic austenite structure, to metallic iron with particle size of $d \geq 10$ – 12 nm and to superparamagnetic at 80 K iron oxides having the diameter 3 – 5 nm $< d < 10$ – 13 nm [10–14].

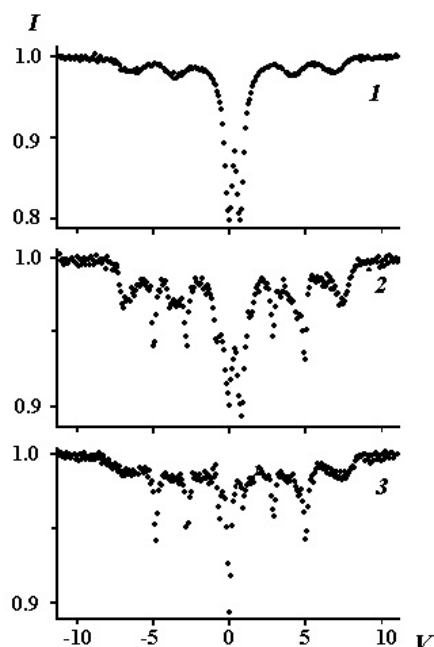


Fig. 1. Mossbauer spectra (80 K) of S1 sample after heat treatment in hydrogen at 350 (1), 550 (2) and 700 °C (3). V – velocity, mm/s; I – relative transmission

Table 1 gives the fitting parameters for the spectra 1–3 with the asymmetric lines of sextet II in the spectra 2–3 being simulated as superposition of two sextets (sextet II.1 and sextet II.2) having Lorentzian line shape. Table 2 gives the relative areas of the subspectra for all the spectra measured with the data being presented in terms of iron distribution between the particles of different sizes and composition. Percentages of iron atoms in the smallest oxide particles ($d < 3$ – 5 nm) in austenite structure and in metallic iron were determined, respectively, as the partial area of doublet, singlet and sextet with $H_{\text{eff}} = 340$ kOe. The difference between the area of the overall spectra and the partial areas of doublet, singlet, and sextet I was attributed to oxide particles with 3 – 5 nm $< d < 10$ – 13 nm.

It can be seen from Table 2 that increase in iron loading leads to increase in particles sizes and in amount of metallic iron, which is a catalyst for carbon hydrogenation reaction [15]. It should be noted, however, that high content of iron oxides in S1 and S2 samples after reduction at 550–700 °C appears to be a result of an oxidation of small iron particles after exposing to air and that in the reducing atmosphere the majority of these particles has to be in a form of metallic iron too. The supports for this conclusion are the known property of iron particles with $d < 10$ nm to be converted into iron oxides by exposing to air, small sizes of oxide particles formed in S1 and S2 samples and our previous data [16–18] on the kinetics of iron oxides reduction in the same activated carbon.

Table 3 gives the total pore volume, those of micro- and mesopores and the surface area of mesopores for starting and hydrogenated carbons, Fig. 2 shows mesopore size distribution curves. As can be seen from Table 3, a rapid activation of iron-containing samples takes place during hydrogen treatment at 550–700 °C. Increase in volume of sorption pores mainly occurs due to mesopores development: the V_{me} , S_{me} values for activated samples are enhanced by a factor of up to 2 compared to the starting carbon. Formation of mesopores with radii $r < 10$ – 11 nm prevails at the initial stages of the samples treatment (Fig. 2) while a growth of larger mesopores a gradual disappearance of micropores and a partial conversion of mesopores into macropores occurs with the proceeding of activation (Fig. 2, Table 3).

Table 1. Mossbauer parameters of the spectra ($T = 80$ K) shown in Figure 1

Spectrum	Subspectra	δ	ΔE_Q	H_{eff}	Γ	Relative area (± 3 %)
		(± 0.05 mm/s)	(± 0.05 mm/s)	(± 3 kOe)	(± 0.05 mm/s)	
1	doublet	0.36	0.83	–	0.63	59
	sextet II	0.36	0.04	455	1.89	41
2	doublet	0.36	0.93	–	0.78	29
	sextet I	0.00	0.01	340	0.38	20
	sextet II.1	0.33	0.06	490	0.68	21
	sextet II.2	0.33	0.14	438	1.58	30
3	doublet	0.36	0.90	–	0.76	3
	singlet	-0.10	–	–	0.29	8
	sextet I	0.00	0.00	338	0.23	18
	sextet II.1	0.47	0.29	483	1.46	28
	sextet II.2	0.10	0.45	309	2.44	43

Table 2. Distribution of iron atoms in iron-containing particles of various size and composition for S1, S2 samples treated in hydrogen at 350–700 °C

Sample	Final heat treatment, 90 min	Percentage of iron atoms in:			
		iron oxides particles, $d < 3-5$ nm	iron oxides particles, $3-5 < d < 10-13$ nm	metallic iron, $d \geq 10-12$ nm	austenite
S1	350 °C	59	41	–	–
	550 °C	29	51	20	–
	700 °C	3	71	18	8
S2	350 °C	64	36	–	–
	550 °C	41	54	5	–
	700 °C	6	83	6	5

Table 3. Some characteristics of porous texture for starting and activated carbons

Sample	Final heat treatment	Burn-off, %	V_{Σ} , cm^3/cm^3	V_{mis} , cm^3/cm^3	V_{me} , cm^3/cm^3	S_{me} , m^2/cm^3
AC	–	0	0.37	0.10	0.09	35
S1	550 °C, 40 min	31	0.41	0.08	0.14	53
	550 °C, 90 min	55	0.47	0.05	0.15	47
	700 °C, 90 min	72	0.50	0.02	0.13	38
S2	550 °C, 90 min	32	0.41	0.10	0.13	55
	550 °C, 90 min	56	0.48	0.08	0.15	65
	700 °C, 90 min	72	0.50	0.02	0.18	70

The data on activation of the S1, S2 samples treated under the same conditions do not reveal a simple relationship between catalyst loading and the percentage of carbon burn-off (Table 3) that appears to be due to the number and complexity of the factors which influence the rate of catalyzed reaction of carbon gasification. At the same time, there is a qualitative correlation between characteristics of catalyst particles and variation in the porous texture of activated samples, namely: in the S2 sample having lower iron content and smaller particles, narrower pores are formed and vice versa. Really, S1 and S2 samples hydrogenated under the same conditions are characterized by practically the same percentages of burn-off (Table 3) and the total pore volume, while at all stages of

activation, S1 samples differ from S2 ones by smaller volume of pores with $r < 8-11$ nm and by greater amount of the broader pores (Fig. 3). With the highest degrees of burn-off (72 %), S2 sample retains well enhanced amount of mesopores compared to the starting carbon, whereas in the case of S1 samples the majority of these pores appears to be converted into macropores (Table 3, Fig. 2 c).

The distinctions in porous texture of S1 and S2 carbon activated under the same conditions to the similar percentages of burn-off can be explained as follows. According to [15], gasification of carbon in catalytic process occurs in the immediate vicinity of catalyst particles, giving rise to the development of pores where the particles are located. Gasification of carbon

with metallic catalyst can be also accompanied by channeling or pitting the carbon substrate [15, 19], with the sizes of the voids being dependent on the sizes of the catalyst particles.

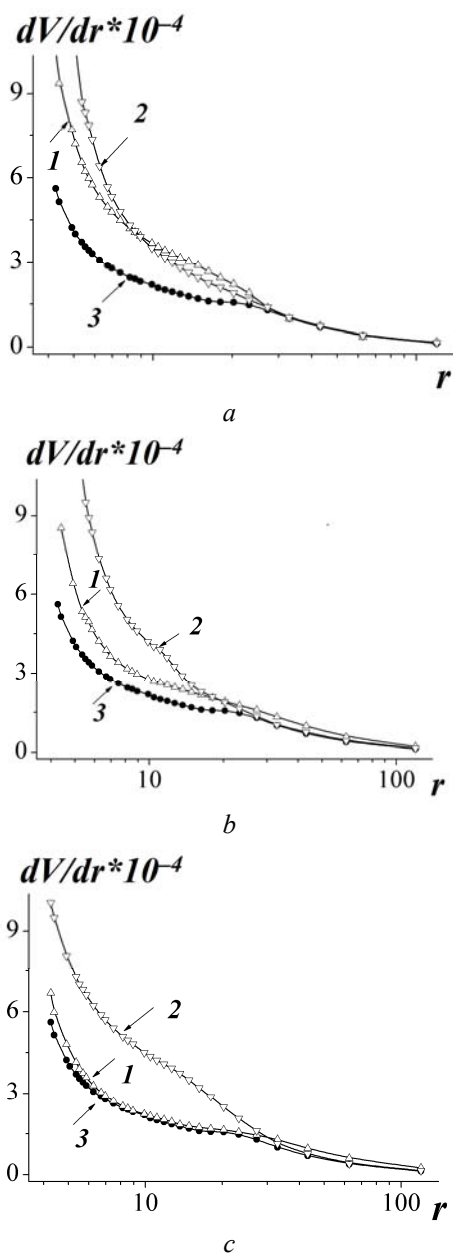


Fig. 2. Mesopore size distribution curves for S1 (1) and S2 (2) samples activated to 31–32 (a), 55–56 (b) and 72 (c) percentages of burn-off. Curve 3 gives mesopore size distribution for starting AC [dV/dr] = cm^2/cm^3 , [r] = nm

Thus, both dispersity of catalyst particles and their distribution in carbon pores must influence the changes in porous texture of activated carbon during hydrogenation. Increase in iron loading leads to an increase in the size and the number of

iron particles that, in turn, may result in increase in the diameter of the voids and in probability for them to coalescence. Another important moment is that enhancement of iron content leads to an increase in amount of catalyst in broad pores. As the rate of reactions in porous solids may depend on sizes of pores and decreases with the pore diameter, the catalyst particles located in wider pores have to play a more important role in carbon gasification. Therefore, a general increase in iron content must result in development of wide pores rather than in growth of narrow ones.

REFERENCES

1. Oya A., Yoshida S., Alcaniz-Monge J., Linares-Solano A. Formation of mesopores in fenolic resin-derived carbon fiber by catalytic activation using cobalt // *Carbon*. – 1995. – V. 33, N 8. – P. 1085–1090.
2. Stavinskaya O.N., Shklovskaya N.I. Variation in the porous structure of iron-containing carbons during hydrogenation // *Rus. J. Phys. Chem.* – 1997. – V. 71, N 9. – P. 1665–1671.
3. Stavinskaya O.N., Shklovskaya N.I. Some peculiarities of the process of activation of synthetic carbons in iron-catalyzed carbon hydrogenation reaction // *Rus. J. Phys. Chem.* – 1999. – V. 72, N 5. – P. 751–755.
4. Burushkina T.N., Aleinikov V.G., Kislitsyn N.A., Myasnikov V.K. A study of the process of the porous structure formation for activated carbon from a copolymer of styrene and divinylbenzene // *Adsorbtsiya i adsorbenty (Adsorption and Adsorbents)*. – 1979. – N 7. – P. 15–19 (in Russian).
5. Dubinin M.M. Fundamentals of the theory of adsorption in micropores of carbon adsorbents: characterization of their adsorption properties and microporous structure // *Carbon*. – 1989. – V. 27, N 3. – P. 457–467.
6. Dubinin M.M., Kataeva L.I. Capillar phenomena and information on porous structure of adsorbents: distribution of mesopore volume and mesopore surface of carbon adsorbents from benzene and nitrogen capillar evaporation experiment // *Izv. Akad. Nauk SSSR, Ser. Khim.* – 1980. – N 3. – P. 498–502 (in Russian).
7. Niemantsverdriet J.W., van der Kraan A.M., Delgass W.N., Vannice M.A. Small particles effects in Mossbauer spectra of a carbon-supported iron catalyst // *J. Phys. Chem.* – 1985. – V. 89, N 1. – P. 67–72.
8. Giessen A.A. Magnetic properties of ultra-fine iron(III) oxide-hydrate particles prepared from iron(III) oxide-hydrate gels // *J. Phys. Chem. Solids*. – 1967. – V. 28, N 2. – P. 343–346.
9. Aharoni S.M., Litt M.H. Superpara-magnetism and exchange anisotropy in microparticles of Fe_3O_4

- embedded in inert carbonaceous matrix // J. Appl. Phys. – 1971. – V. 42, N 1. – P. 352–357.
10. Roggwiller P., Kundig W. Mossbauer spectra of superparamagnetic Fe₃O₄ // Solid State Commun. – 1973. – V. 12, N 9. – P. 901–903.
 11. Maneda Y., Aramaki M., Takashima Y. et al. Mossbauer study of iron oxide layers formed on fine iron particles // Bull. Chem. Soc. Jpn. – 1987. – V. 60, N 11. – P. 3241–3246.
 12. McNab T.K., Fox R.A., Bovie A.J.F. Some magnetic properties of magnetite (Fe₃O₄) microcrystals // J. Appl. Phys. – 1972. – V. 39, N 12. – P. 5703–5711.
 13. Suzdalev I.P. On superparamagnetism of ultrafine antiferromagnetic particles // Fiz. Tverd. Tela. – 1970. – V. 12, N 4. – P. 988–990 (in Russian).
 14. Haneda K., Morrish A.H. Vacancy ordering in γ -Fe₂O₃ small particles // Solid State Commun. – 1977. – V. 22, N 12. – P. 779–782.
 15. McKee D.W. The catalyzed gasification reactions of carbon // Chemistry and Physics of Carbon / Walker Jr. PL, Throver PA., eds. New York: Marcell Dekker, 1981. – V. 16. – P. 1–121.
 16. Stavinskaya O.N., Imshennik V.K., Oranskaya E.I. et al. Dispersity and composition of iron-containing particles in adsorbents prepared from synthetic active carbons // Rus. J. Phys. Chem. – 1998. – V. 72, N 7. – P. 1138–1143.
 17. Stavinskaya O.N., Imshennik V.K. Structure of iron-containing particles deposited on carbon as studied by Mossbauer spectroscopy // Rus. J. Phys. Chem. – 2000. – V. 74, N 11. – P. 2107–2112.
 18. Stavinskaya O.N., Imshennik V.K. The reduction of iron-containing particles deposited on carbon under the conditions of iron-catalyzed carbon hydrogenation. // Rus. J. Phys. Chem. – 2006. – V. 80, N 12. – P. 1925–1928.
 19. Chu X., Schmidt L.D. Gasification of graphite studied by scanning tunneling microscopy // Carbon. – 1991. – V. 29, N 8. – P. 1251–1255.

Received 19.10.2012, accepted 18.01.2013

Взаємозв'язок між характеристиками частинок каталізатора та зміною пористої структури активного вугілля в каталізованій залізом реакції гідрогенізації вуглецю

О.М. Ставинська

*Институт хімії поверхні ім. О.О. Чуйка Національної академії наук України
вул. Генерала Наумова, 17, Київ, 03164, Україна, okstavinskaya@yahoo.com*

Методом мессбауерівської спектроскопії вивчено склад і розміри залізовмісних частинок, що формуються в порах активного вугілля при термообробці в атмосфері водню. Адсорбційним методом досліджено зміну пористої структури вугілля внаслідок каналізованої залізом реакції гідрогенізації вуглецю. Знайдено, що при однакових значеннях обгару розміри пор, що формуються в адсорбенті при активуванні, збільшуються у зразка з більшим вмістом заліза і з більшими розмірами частинок каталізатора.

Взаимосвязь между характеристиками частиц катализатора и изменением пористой структуры активного угля в катализируемой железом реакции гидрогенизации углерода

О.Н. Ставинская

*Институт химии поверхности им. А.А. Чуйко Национальной академии наук Украины
ул. Генерала Наумова, 17, Киев, 03164, Украина, okstavinskaya@yahoo.com*

Методом мессбауэровской спектроскопии изучены состав и размеры железосодержащих частиц, образующихся в порах активного угля в процессе термообработки в атмосфере водорода. Адсорбционным методом изучено изменение пористой структуры активного угля в результате катализируемой железом реакции гидрогенизации углерода. Обнаружено, что при одинаковых значениях обгара размеры пор, образующихся в адсорбенте при активировании, увеличиваются для образца с большим содержанием железа и с большими размерами частиц катализатора.